



ROTATIONAL INERTIA FORCE EFFECTS IN CIRCULAR SQUEEZE FILMS WITH A NON-NEWTONIAN FERROFLUID

Jaw-Ren Lin

Department of Mechanical Engineering, Nanya Institute of Technology, Taoyuan, Taiwan, R.O.C., jrlin@nanya.edu.tw

Li-Ming Chu

Interdisciplinary Program of Green and Information Technology, Department of Applied Science, National Taitung University, Taitung, Taiwan, R.O.C.

Long-Jin Liang

Department of Mechanical Engineering, Nanya Institute of Technology, Taoyuan, Taiwan, R.O.C.

Shu-Ting Hu

Department of Mechanical Engineering, Nanya Institute of Technology, Taoyuan, Taiwan, R.O.C.

Follow this and additional works at: <https://jmstt.ntou.edu.tw/journal>



Part of the [Engineering Commons](#)

Recommended Citation

Lin, Jaw-Ren; Chu, Li-Ming; Liang, Long-Jin; and Hu, Shu-Ting (2018) "ROTATIONAL INERTIA FORCE EFFECTS IN CIRCULAR SQUEEZE FILMS WITH A NON-NEWTONIAN FERROFLUID," *Journal of Marine Science and Technology*. Vol. 26 : Iss. 4 , Article 11.

DOI: 10.6119/JMST.201808_26(4).0011

Available at: <https://jmstt.ntou.edu.tw/journal/vol26/iss4/11>

This Research Article is brought to you for free and open access by Journal of Marine Science and Technology. It has been accepted for inclusion in Journal of Marine Science and Technology by an authorized editor of Journal of Marine Science and Technology.

ROTATIONAL INERTIA FORCE EFFECTS IN CIRCULAR SQUEEZE FILMS WITH A NON-NEWTONIAN FERROFLUID

Jaw-Ren Lin¹, Li-Ming Chu², Long-Jin Liang¹, and Shu-Ting Hu¹

Key words: rotating disks, ferrofluids, non-Newtonian couple stresses, squeeze films.

ABSTRACT

This paper aims to investigate the effects of rotational inertia force on the squeeze film characteristics between two circular disks lubricated with a non-Newtonian ferrofluid. Based on the Shliomis ferromagnetic fluid model incorporating with the Stokes couple stress fluid model, we have derived a non-Newtonian ferromagnetic Reynolds equation including the rotational inertia force effects for the study of squeeze film performances. From the results, the effects of rotational inertia forces of the upper disk yield a lower load capacity and a shorter squeezing time as compared to the non-rotating case. In addition, the influences of the related parameters on the squeeze film characteristics are also included in Table 1 for engineering applications.

I. INTRODUCTION

Squeeze film techniques arises between two fluid-contained surfaces approaching each other with a normal velocity. The load-carrying capacity and the separated gap are then measured. Owing to the gap cushion, squeeze film mechanisms are widely applied in many areas of engineering practices, such as the artificial lubricated joints, molding injection machinery, hydrodynamic dampers, automatic transmission units, clutch pads, and machine tool systems. With the development of modern engineering, the increasing use of ferrofluids, also named magnetic fluids, has received international attention. Based on the contributions of Shliomis (1972, 1974), ferrofluids are prepared by suspending ferromagnetic particles coated with surfactant dispersing in a liquid carrier. Under the action of an external magnetic field, each ferromagnetic particle can experience a body

force which causes it to move to some preferred locations. Because of their peculiar characteristics, ferrofluids possess a variety of engineering applications, such as the magnetic drug targeting for tumour treatment of Odenbach and Gitter (2011), the novel optical devices of Zhal et al. (2011), the microfluidic pumps and valves of Hartshorne et al. (2004), and the servo-valve torque motors of Li and Song (2007). Furthermore, ferrofluids can also be applied to hydrodynamic squeeze film bearings. For example, Shah and Bhat (2005) investigated the squeeze film between exponential curved plates. The effects of ferrofluids and the curvature of plates on the squeeze film performances are discussed by Shah and Bhat (2005). Lin (2013) studied the squeeze film characteristics between a sphere and a plate lubricated with a ferrofluid. The influences of convective fluid inertia forces are also included in the discussion. From the results obtained by Lin (2013), the effects of ferrofluids in the presence of external magnetic fields provide a higher load capacity as well as a longer response time for the squeeze film. In order to adjust some physical and chemical properties, the lubricants in squeeze films often contain small amount of additives of long-chain organic compounds. In this situation, the Newtonian postulate neglecting the size of fluid particles is no longer a satisfactory approach to the non-Newtonian lubricants in squeeze films. In order to describe the peculiar behaviors of these kinds of non-Newtonian fluids, a micro-continuum theory has been proposed by Stokes (1966). The Stokes micro-continuum theory is the simplest generation that takes into account the presence of couple stresses and body couples. A number of investigators have applied the Stokes micro-continuum theory of couple stress fluid model to study the squeeze film characteristics between approaching surfaces, such as the squeeze films with reference to human joints by Bujurke and Jayaraman (1982) and Ahmad and Singh (2007), the squeeze films between a non-rotating shaft and a cylindrical shell by Lin (1998), and the squeeze films between a sphere and a plate by Elsharkawy and AL-Fadhlah (2008) and Lin (2000). According to their results, the influences of non-Newtonian couple stresses provide an increased value in the load capacity and the response time as compared to the case with a Newtonian fluid. Recently, Lin et al. (2013) investigated the squeeze film characteristics between non-rotating circular disks lubricated with non-Newtonian couple-stress fer-

Paper submitted 05/13/16; revised 08/25/16; accepted 06/25/18. Author for correspondence: Jaw-Ren Lin (e-mail: jrlin@nanya.edu.tw).

¹ Department of Mechanical Engineering, Nanya Institute of Technology, Taoyuan, Taiwan, R.O.C.

² Interdisciplinary Program of Green and Information Technology, Department of Applied Science, National Taitung University, Taitung, Taiwan, R.O.C.

rofluids. It is found that the effects of non-Newtonian ferrofluids provide a higher load capacity and a longer response time as compared to the Newtonian non-ferrofluid case. However, the study of squeeze film characteristics between rotating circular disks lubricated with non-Newtonian couple-stress ferrofluids is still absent. Therefore, a further investigation on the rotating circular squeeze film with non-Newtonian ferrofluids is of interest.

The purpose of the present study is to investigate the effects of rotational inertia force on the squeeze film characteristics between circular disks lubricated with a non-Newtonian ferrofluid in the presence of a transverse magnetic field. Based on the Shliomis ferromagnetic fluid model incorporating with the Stokes couple stress fluid model, a non-Newtonian ferromagnetic Reynolds equation including the effects of rotational inertia force will be derived for the study of squeeze film performances. As compared to the Newtonian non-ferrofluid non-inertia case, the squeeze film characteristics between rotating circular disks lubricated with non-Newtonian ferrofluids are presented and discussed through the variation of the non-Newtonian parameter, the concentration parameter, the Langevin magnetic parameter and the rotational inertia parameter, respectively.

II. ANALYSIS

Fig. 1 shows the squeeze film geometry for rotating circular disks of radius A under the application of a constant magnetic field $\vec{B} = (0, 0, B_0)$. The upper rotating disk with angular speed Ω is approaching the lower one with a squeezing velocity $(-dh/dt)$, where t is the time and h denotes the film thickness. The lubricant in the film region is taken to be an incompressible non-Newtonian ferrofluid. Based on the ferromagnetic fluid model of Shliomis (1972, 1974) incorporating the micro-continuum theory of couple stress fluid model of Stokes (1966), the Maxwell equations, the continuity equation, and the momentum equations can be expressed in a vector form.

$$\nabla \times \vec{B} = 0 \tag{1}$$

$$\nabla \cdot (\vec{B} + \vec{M}) = 0 \tag{2}$$

$$\nabla \cdot \vec{v} = 0 \tag{3}$$

$$\rho \frac{D\vec{v}}{Dt} = -\nabla p + \eta \nabla^2 \vec{v} + \mu_0 (\vec{M} \cdot \nabla) \vec{B} + \mu_0 \nabla \times (\vec{M} \times \vec{B}) / 2 - \eta_n \nabla^4 \vec{v} \tag{4}$$

where

$$\vec{M} = \frac{M_e}{B_0} \left\{ \vec{B} + \frac{3\eta C [(\nabla \times \vec{v}) \times \vec{B}]}{n B_c \Gamma (1 + L \coth L)} \right\} \tag{5}$$

$$M_e = mn (\coth L - 1/L) \tag{6}$$

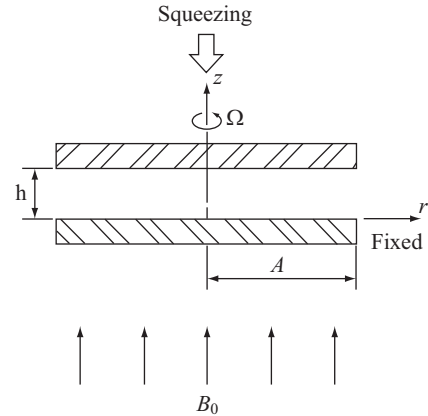


Fig. 1. Rotating circular squeeze film disks lubricated with a non-Newtonian ferrofluid in the presence of applied magnetic fields.

In the above equations, \vec{v} is the fluid velocity, ρ is the fluid density, η is the viscosity of the suspension, η_n is a new material constant responsible for the non-Newtonian properties of couple stress fluids, μ_0 is the free space permeability, \vec{M} is the magnetization vector, M_e is the equilibrium magnetization, m is the magnetic moment of a particle, n is the number of particles per unit volume, B_c is the Boltzmann constant, Γ is the absolute temperature, C is the volume concentration of ferromagnetic particles, and L is the Langevin magnetic parameter,

$$L = \frac{m\mu_p B_0}{B_c \Gamma} \tag{7}$$

Assume that the thin-film lubrication theory is applicable for the present analysis, the body force and the body couples are negligible, but the rotational inertia forces due to the upper rotational disk are considered. Substituting Eq. (5) into Eq. (4) and performing the analysis of the order of magnitude, the continuity equation and the momentum equations for an axially symmetric flow can be reduced as follows.

$$\frac{u}{r} + \frac{\partial u}{\partial r} + \frac{\partial w}{\partial z} = 0 \tag{8}$$

$$\eta_n \frac{\partial^4 u}{\partial z^4} - \eta \frac{\partial^2 u}{\partial z^2} - \left(\frac{3}{2} C \frac{L - \tanh L}{L + \tanh L} \right) \eta \frac{\partial^2 u}{\partial z^2} = -\frac{\partial p}{\partial r} + \frac{\rho v^2}{r} \tag{9}$$

$$\eta_n \frac{\partial^4 v}{\partial z^4} - \eta \frac{\partial^2 v}{\partial z^2} = 0 \tag{10}$$

$$\frac{\partial p}{\partial z} = 0 \tag{11}$$

where the symbols u , v and w denote the velocity components in the r -, θ and z - directions, respectively. According to the re-

search of Batchelor (1977), the viscosity of suspension increases with the volume fraction of ferromagnetic particles, $\eta = \eta_0\Phi$.

$$\Phi = 1 + \frac{5}{2}C + \frac{31}{5}C^2 \tag{12}$$

where η_0 denotes the viscosity of the liquid carrier. The non-slip velocity conditions and the non-couple stress conditions at the solid boundaries are

$$u(z = 0) = 0, u(z = h) = 0 \tag{13a}$$

$$\left. \frac{\partial^2 u}{\partial z^2} \right|_{z=0} = 0, \left. \frac{\partial^2 u}{\partial z^2} \right|_{z=h} = 0 \tag{13b}$$

$$v(z = 0) = 0, v(z = h) = r\Omega \tag{14a}$$

$$\left. \frac{\partial^2 v}{\partial z^2} \right|_{z=0} = 0, \left. \frac{\partial^2 v}{\partial z^2} \right|_{z=h} = 0 \tag{14b}$$

$$w(z = 0) = 0, w(z = h) = \frac{dh}{dt} \tag{15}$$

Integrating Eq. (10) with respect to z subject to the conditions (14a) and (14b), one can obtain the circumferential velocity component, v .

$$v = \frac{r\Omega}{h} z \tag{16}$$

Substituting the expression of v into Eq. (9) and integrating the equation subject to the conditions (13a) and (13b), one can obtain the radial velocity component, u .

$$u = \frac{1}{2\eta_0\Phi(1+\tau)} \frac{\partial p}{\partial r} \left\{ \begin{aligned} & z^2 - hz + \frac{2l_c^2}{\Phi(1+\tau)} \\ & \cdot \left[1 - \frac{\cosh\left[\frac{(z-0.5h)\sqrt{\Phi(1+\tau)}}{l_n}\right]}{\cosh\left[\frac{0.5h\sqrt{\Phi(1+\tau)}}{l_n}\right]} \right] \end{aligned} \right\} + \frac{\rho\Omega^2 r}{12\eta_0\Phi(1+\tau)h^2} \left\{ \begin{aligned} & -z^4 - \frac{12l_c^2}{\Phi(1+\tau)} \\ & \cdot \left[z^2 - h^2 - \frac{\sinh\left[\frac{z\sqrt{\Phi(1+\tau)}}{l_n}\right]}{\sinh\left[\frac{h\sqrt{\Phi(1+\tau)}}{l_n}\right]} \right] \\ & + h^3 z - \frac{24l_c^4}{\Phi^2(1+\tau)^2} \\ & \cdot \left[1 - \frac{\cosh\left[\frac{(z-0.5h)\sqrt{\Phi(1+\tau)}}{l_n}\right]}{\cosh\left[\frac{0.5h\sqrt{\Phi(1+\tau)}}{l_n}\right]} \right] \end{aligned} \right\} \tag{17}$$

where

$$\tau = \frac{3}{2}C \frac{L - \tanh L}{L + \tanh L} \tag{18}$$

$$l_n = \sqrt{\eta_n / \eta_0} \tag{19}$$

Integrating the continuity Eq. (8) across the film thickness and applying the velocity boundary conditions of u and w , one can derive a modified Reynolds equation.

$$\frac{1}{r} \frac{\partial}{\partial r} \left\{ \begin{aligned} & f_A(h, l_n, \Phi, \tau) r \frac{dp}{dr} \\ & - \frac{3\rho\Omega^2}{10} f_B(h, l_n, \Phi, \tau) r^2 \end{aligned} \right\} = 12\eta_0\Phi(1+\tau) \frac{dh}{dt} \tag{20}$$

where

$$f_A = h^3 - \frac{12l_n^2}{\Phi(1+\tau)} \left\{ h - \frac{2l_n}{\sqrt{\Phi(1+\tau)}} \tanh \left[\frac{h\sqrt{\Phi(1+\tau)}}{2l_n} \right] \right\} \tag{21}$$

$$f_B = \left\{ \begin{aligned} & h^3 - \frac{40l_n^2}{3\Phi(1+\tau)} h \\ & + \frac{40l_n^3}{[\Phi(1+\tau)]^{3/2}} \tanh \left[\frac{h\sqrt{\Phi(1+\tau)}}{2l_n} \right] \\ & - \frac{80l_n^4}{[\Phi(1+\tau)]^2} \frac{1}{h} \\ & + \frac{160l_n^5}{[\Phi(1+\tau)]^{5/2}} \frac{1}{h^2} \tanh \left[\frac{h\sqrt{\Phi(1+\tau)}}{2l_n} \right] \end{aligned} \right\} \tag{22}$$

This derived Reynolds equation can be applied to the study of rotating circular squeeze films lubricated with a non-Newtonian ferrofluid including the fluid inertia force effects due to the upper rotational disk. Introduce non-dimensional parameter and variables as follows.

$$r^* = \frac{r}{A}, h^* = \frac{h}{h_0}, p^* = \frac{ph_0^3}{\eta_0 A^2 (-dh/dt)} \tag{23}$$

$$f_A^* = \frac{f_A}{h_0^3}, f_B^* = \frac{f_B}{h_0^3} \tag{24}$$

$$R = \frac{\rho h_0^3 \Omega^2}{\eta_0 (-dh/dt)}, N = \frac{l_n}{h_0} \tag{25}$$

where h_0 denotes the initial film thickness. As a result, the modified Reynolds equation can be expressed in a non-dimensional form.

$$f_A^* \cdot \frac{1}{r^*} \frac{d}{dr^*} \left\{ r^* \frac{dp^*}{dr^*} \right\} = \frac{3R}{5} \cdot f_B^* - 12\Phi(1+\tau) \quad (26)$$

where

$$f_A^* = h^{*3} - \frac{12N^2}{\Phi(1+\tau)} \cdot \left[h^* - \frac{2N}{\sqrt{\Phi(1+\tau)}} \tanh \left[\frac{h^* \sqrt{\Phi(1+\tau)}}{2N} \right] \right] \quad (27)$$

$$f_B^* = \left\{ \begin{array}{l} h^{*3*} - \frac{40N^2}{3\Phi(1+\tau)} h^* \\ + \frac{40N^3}{[\Phi(1+\tau)]^{3/2}} \tanh \left[\frac{h^* \sqrt{\Phi(1+\tau)}}{2N} \right] \\ - \frac{80N^4}{[\Phi(1+\tau)]^2} \frac{1}{h^*} \\ + \frac{160N^5}{[\Phi(1+\tau)]^{5/2}} \frac{1}{h^{*2}} \tanh \left[\frac{h^* \sqrt{\Phi(1+\tau)}}{2N} \right] \end{array} \right\} \quad (28)$$

Once the film pressure is obtained, the squeeze film performances can be evaluated.

III. SQUEEZE FILM CHARACTERISTICS

The non-dimensional pressure boundary conditions are: $p^* = 0$ at $r^* = 1$; and $dp^*/dr^* = 0$ at $r^* = 0$. Integrating the non-dimensional Reynolds equation subject to the pressure boundary conditions, one can obtain the non-dimensional film pressure.

$$p^* = \frac{60\Phi(1+\tau) - 3Rf_B^*}{20f_A^*} (1-r^{*2}) \quad (29)$$

The load capacity is evaluated by integrating the film pressure over the disk surface.

$$W = 2\pi \int_{r=0}^A pr dr \quad (30)$$

Introducing the non-dimensional variable, the above equation can be written as:

$$W^* = \frac{Wh_0^3}{\eta_0 A^4 (-dh/dt)} = 2\pi \int_{r^*=0}^1 p^* r^* dr^* \quad (31)$$

Applying the expression of the non-dimensional film pressure and performing the integration, one can obtain the non-dimensional load capacity.

$$W^* = \frac{60\pi\Phi(1+\tau) - 3\pi Rf_B^*}{40f_A^*} \quad (32)$$

The local film height h at the time t can be obtained by solving Eq. (31) for prescribed initial conditions, and prescribed loads and angular speeds. In the present study, a time-independent load and a constant rotating speed are considered as Prakash and Tiwari (1985). For a time-independent load and a constant rotating speed, the time $\Delta t = t_1 - t_0$ taken by the upper disk to move from h_0 to h_1 is obtained by integrating Eq. (31) with respect to time. Since $W^* = Wh_0^3 / \eta_0 A^4 (-dh/dt)$, one can introduce the non-dimensional squeeze film time:

$$t^* = \frac{Wh_0^2}{\eta_0 A^4} \cdot t \quad (33)$$

Then the time-height relationship can be described as the following non-dimensional form.

$$\frac{dh^*}{dt^*} = - \frac{40f_A^*}{60\pi\Phi(1+\tau) - 3\pi Rf_B^*} \quad (34)$$

Separating the variables and integrating the equation give

$$\Delta t^* = \pi \cdot \int_{h^*=1}^{h^*} \frac{60\Phi(1+\tau) - 3Rf_B^*}{40f_A^*} dh^* \quad (35)$$

The squeeze film time can be numerically calculated by the Gaussian Quadrature method.

IV. RESULTS AND DISCUSSION

Based on the above analysis, the squeeze film performances between rotating circular disks lubricated with non-Newtonian ferrofluids are characterized by the rotational inertia parameter R , the non-Newtonian parameter N , the volume concentration of ferromagnetic particles C , and the Langevin magnetic parameter L . Several special cases can be included from the limiting values of these parameters.

Case 1: $R = 0, N = 0, C = 0, L = 0$:

The non-dimensional film pressure in Eq. (29) reduces to

$$\lim_{\substack{R \rightarrow 0, N \rightarrow 0 \\ C \rightarrow 0, L \rightarrow 0}} p^* = \frac{3(1-r^{*2})}{h^{*3}} \quad (36)$$

It is the case of squeeze films between non-rotating disks with Newtonian non-ferrofluids by Hamrock (1994).

Case 2: $R \neq 0, N \neq 0, C = 0, L = 0$:

The non-dimensional Reynolds equation in Eq. (26) reduces to

$$f^* \cdot \frac{1}{r^*} \frac{d}{dr^*} \left\{ r^* \frac{dp^*}{dr^*} \right\} = g \cdot R - 12 \quad (37)$$

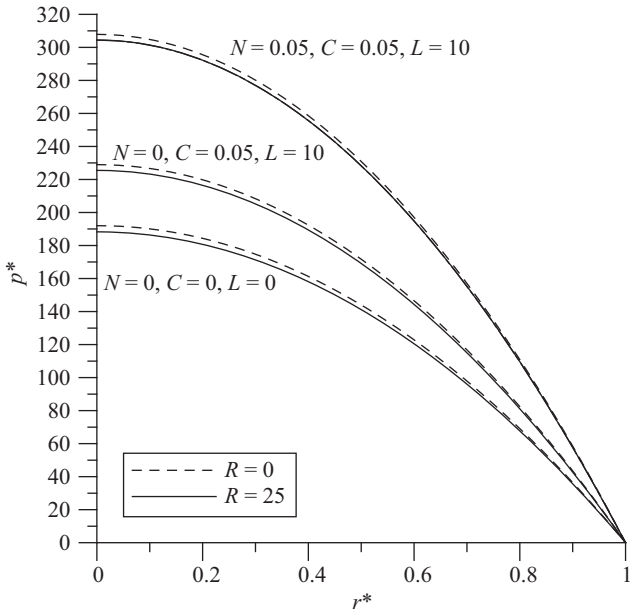


Fig. 2. Non-dimensional squeeze film pressure p^* as a function of the non-dimensional radial position r^* at the non-dimensional film height $h^* = 0.25$ for various N, C, L and R .

where

$$f^* = h^{*3} - 12N^2h^* + 24N^3 \tanh(h^*/2N) \quad (38)$$

$$g^* = \left\{ \begin{array}{l} 0.6h^{*3} - 8N^2h^* + 24N^3 \tanh(h^*/2N) \\ -48N^4/h^* + 96(N^5/h^{*2}) \tanh(h^*/2N) \end{array} \right\} \quad (39)$$

It is the case of squeeze films between non-rotating disks with non-Newtonian non-ferrofluids by Lin and Hung (2008).

Case 3: $R = 0, N \neq 0, C \neq 0, L \neq 0$:

The non-dimensional load capacity in Eq. (32) reduces to

$$\lim_{R \rightarrow 0} W^* = \frac{3\pi\Phi(1+\tau)}{2f_A^*} \quad (40)$$

It is the case of squeeze films between non-rotating disks with non-Newtonian ferrofluids of Lin et al. (2013).

In the present study, the parameters for the squeeze film characteristics are illustrated as follows: $R = 0 - 25, N = 0 - 0.05, C = 0 - 0.05, L = 0 - 10$.

Fig. 2 shows the non-dimensional squeeze film pressure p^* as a function of the non-dimensional radial position r^* at the film height $h^* = 0.25$ for various values of N, C, L and R . In the situation of non-rotating disks ($R = 0$), the squeeze film with a Newtonian ferrofluid under the action of an external magnetic field ($N = 0, C = 0.05, L = 10$) is observed to provide a higher film pressure as compared to the case of a Newtonian non-ferrofluid without magnetic fields ($N = 0, C = 0, L = 0$). When the effects of non-Newtonian rheology ($N = 0.05, C = 0.05, L =$

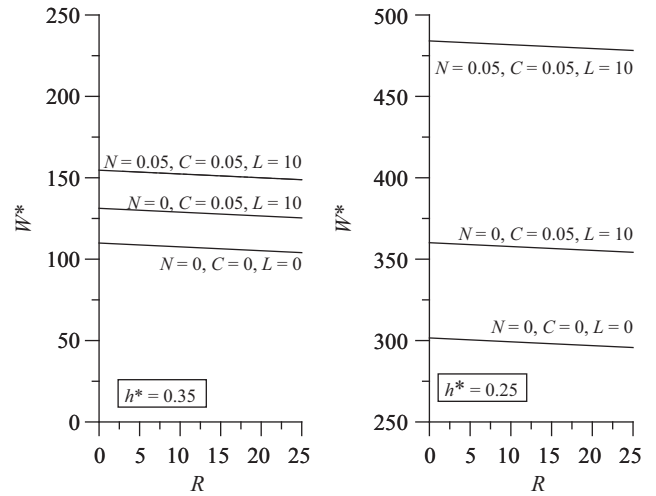


Fig. 3. Non-dimensional load capacity W^* as a function of the rotational inertia parameter R at the non-dimensional film height $h^* = 0.35$ and 0.25 for various N, C and L .

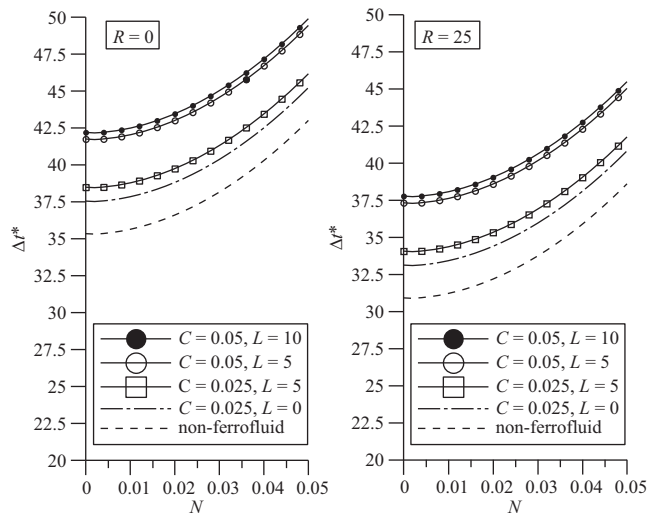


Fig. 4. Non-dimensional squeeze film time Δt^* as a function of N under $h = 0.25$ without rotational inertia ($R = 0$) and with rotational inertia ($R = 25$)

10) are included, further higher values of the pressure are obtained. In addition, the effects of rotational inertia force ($R = 25$) due to the upper rotating disk result in a decreased film pressure as compared to the non-rotating case ($R = 0$).

Fig. 3 presents the non-dimensional load capacity W^* as a function of the rotational inertia parameter R at the non-dimensional film height $h^* = 0.35$ and 0.25 for various values of N, C and L . Since the squeeze film with rotational inertia forces results in a lower pressure as compared to the non-inertia case, the integrated loads are similarly affected. At the non-dimensional film height $h^* = 0.35$, the load capacity decreases with increasing values of the rotational inertia parameter. Furthermore, the effects of rotational inertia force on the load capacity are more pronounced for the squeeze film operating at a lower film height $h^* = 0.25$.

Table 1. Non-dimensional load capacity W^* of non-Newtonian ferrofluid lubricated rotating circular disks for various values of N , C , L and R at the non-dimensional film height $h^* = 0.5$.

Non-dimensional load capacity W^*				
$L = 0$				
N	C	$R = 0$	$R = 15$	$R = 25$
0	0	37.6991 (Hamrock, 1994)	-	-
0	0.02	37.6991	34.1648	31.8086
0.02	0.02	39.5841	36.0498	33.6936
0.04	0.02	40.2628	36.7330	34.3798
0.04	0.02	42.1880	38.6651	36.3165
0.04	0.04	44.0769	40.5537	38.2049
$L = 5$				
N	C	$R = 0$	$R = 15$	$R = 25$
0	0	37.6991	34.1648	31.8086
0	0.02	40.3758	36.8415	34.4853
0.02	0.02	41.0549	37.5250	35.1718
0.04	0.02	42.9814	39.4584	37.1097
0.04	0.04	45.7391	42.2157	39.8667
$L = 10$				
N	C	$R = 0$	$R = 15$	$R = 25$
0	0	37.6991	34.1648	31.8086
0	0.02	40.5557	37.0214	34.6652
0.02	0.02	41.2349	37.7050	35.3517
0.04	0.02	43.1617	39.6386	37.2899
0.04	0.04	46.1168	42.5933	40.2443
		46.1168 (Lin et al., 2013)	-	-

Fig. 4 shows the non-dimensional squeeze film time Δt^* as a function of the non-Newtonian parameter N for various C and L at the non-dimensional film height $h^* = 0.25$ without rotational inertia ($R = 0$) and with rotational inertia ($R = 25$), respectively. The squeeze film time Δt^* is observed to increase with increasing values of the non-Newtonian parameter N . For the non-inertia squeeze film ($R = 0$), it is observed that the use of ferrofluids ($C = 0.05$ or $C = 0.025$) with or without magnetic fields ($L = 5$ or $L = 0$) yields a longer squeeze film time as compared to the non-ferrofluid case. However, when the rotation of upper disk is included, the effects of rotational inertia force ($R = 25$) predict shorter values of the squeeze film time as compared to the non-rotating case ($R = 0$).

In order to guide the use of the present study, an example of calculating the values of the rotational inertia parameter R and the non-Newtonian parameter N is illustrated as follows.

The volume of ferromagnetic particles including surfactants is $4.1667 \times 10^{-5} \text{ m}^3$, the volume of the main liquid is $1.00 \times 10^{-3} \text{ m}^3$; and:

$$\begin{aligned}
 A &= 0.05 \text{ m}, h_0 = \times 10^{-4} \text{ m}, \Omega = 1000 \text{ rpm}, \\
 -dh/dt &= 2.5 \times 10^{-3} \text{ m} \cdot \text{s}^{-1}, \rho = 900 \text{ kg} \cdot \text{m}^{-3}, \\
 \eta_n &= 1.2325 \times 10^{-12} \text{ kg} \cdot \text{m} \cdot \text{s}^{-1}, \Gamma = 298 \text{ K}, \\
 m &= 2 \times 10^{-19} \text{ Amp} \cdot \text{m}^2, \\
 \mu_p &= 4\pi \times 10^{-7} \text{ kg} \cdot \text{m} \cdot \text{s}^{-2} \cdot \text{Amp}^{-2}, \\
 B_0 &= 1.6363 \times 10^5 \text{ Amp} \cdot \text{m}^{-1}, \\
 B_c &= 1.38 \times 10^{-23} \text{ kg} \cdot \text{m}^2 \cdot \text{s}^{-2} \cdot \text{K}^{-1}.
 \end{aligned}$$

According to the definitions in **ANALYSIS**, the rotational inertia parameter, the non-Newtonian parameter, the volume concentration of ferromagnetic particles, and the Langevin magnetic parameter can be obtained:

$$R = 25, N = 0.05, C = 0.04, L = 10.$$

Table 1 shows some numerical values of the non-dimensional squeeze film load capacity of non-Newtonian ferrofluid lubricated rotating circular disks at the half film height. It is observed that increasing the rotational inertia parameter decreases the load capacity of non-Newtonian ferrofluid lubricated squeeze films.

V. CONCLUSIONS

In this paper, we have investigated the effects of rotational inertia force on the squeeze film characteristics between two circular disks lubricated with a non-Newtonian ferrofluid in the presence of a transverse magnetic field. Based on the Shliomis ferromagnetic fluid model incorporating with the Stokes couple stress fluid model, a non-Newtonian ferromagnetic Reynolds equation including the effects of rotational inertia force has been derived for the study of squeeze film performances. Several special cases can be included from the limiting values of these parameters. It is shown that the effects of rotational inertia force of circular disks lubricated with a non-Newtonian ferrofluid result in a lower load capacity and a shorter squeeze film time as compared to the non-inertia case. Some numerical values of the non-dimensional squeeze film load capacity varying with the rotational inertia parameter, the non-Newtonian parameter, the

volume concentration parameter, and the Langevin magnetic parameter are also provided in Table 1 for engineering applications.

ACKNOWLEDGEMENTS

The present study is supported by the Ministry of Science and Technology of Republic of China: MOST 104-2221-E-253-005-

REFERENCES

- Ahmad N. and J. P. Singh (2007). A model for couple-stress fluid film mechanism with reference to human joint. *Proceedings of the IMechE PartJ: Journal of Engineering Tribology* 221, 755-759.
- Batchelor, G. K. (1977). The effect of Brownian motion on the bulk stress in a suspension of spherical particles. *Journal of Fluid Mechanics* 83, 97-117.
- Bujurke, N. M. and G. Jayaraman (1982). The Influence of couple stresses in squeeze films. *International Journal of Mechanical Science* 24, 369-376.
- Elsharkawy A. A. and K. J. AL-Fadhlah (2008). Separation of a sphere from a flat in the presence of couple stress fluids. *Lubrication Science* 20, 61-74.
- Hamrock, B. J. (1994). *Fundamentals of Fluid Film Lubrication*. McGraw-Hill, 286-287.
- Hartshorne, H., C. J. Backhouse and W. E. Lee (2004). Ferrofluid-based microchip pump and valve. *Sensors and Actuators B* 99, 592-600.
- Li, S. and Y. Song (2007). Dynamic response of a hydraulic servo-valve torque motor with magnetic fluids. *Mechatronics* 17, 442-447.
- Lin J. R. (1998). Squeeze film characteristics of finite journal bearings: couple stress fluid model. *Tribology International* 31, 201-207.
- Lin, J. R. (2000). Squeeze film characteristics between a sphere and a flat plate: couple stress fluid model. *Computers and Structures* 75, 73-80.
- Lin, J. R. (2013). Fluid inertia effects in ferrofluid squeeze film between a sphere and a plate. *Applied Mathematical Modelling* 37, 5528-5535.
- Lin, J. R. and C. R. Hung (2008). Combined effects of non-Newtonian rheology and rotational inertia on the squeeze film characteristics of parallel circular discs. *Journal of Engineering Tribology* 222, 629-636.
- Lin J. R., R. F. Lu, M. C. Lin and P. Y. Wang (2013). Squeeze film characteristics of parallel circular disks lubricated by ferrofluids with non-Newtonian couple stresses. *Tribology International* 61, 56-61.
- Odenbach, S. and K. Gitter (2011). Experimental investigations on a branched tube model in magnetic drug targeting. *Journal of Magnetism and Magnetic Materials* 323, 1413-1416.
- Prakash, J. and K. Tiwari (1985). Effect of surface roughness on the squeeze film between rotating porous annular disks with arbitrary porous wall thickness. *International Journal Mechanical Sciences* 27, 135-144.
- Shah, R. C. and M. V. Bhat (2005). Ferrofluid squeeze film between curved annular plates including rotation of magnetic particles. *Journal of Engineering Mathematics* 51, 317-324.
- Shliomis, M. I. (1972). Effective viscosity of magnetic suspensions. *Soviet Physics JETP* 34, 1291-1294.
- Shliomis, M. I. (1974). Magnetic fluids. *Soviet Physics Usp* 17, 153-169.
- Stokes, V. K. (1966). Couple stresses in fluids. *Physics of Fluids* 9, 1709-1715.
- Zhao, Y., Y. Zhang, R. Lv and Q. Wang (2011). Novel optical devices based on the tunable refractive index of magnetic fluid and their characteristics. *Journal of Magnetism and Magnetic Materials* 323, 2987-2996.